Available online at www.sciencedirect.com
ScienceDirect
Journal of Power Sources 159 (2006) 461–467
JOURNAL OF POWER SOURCES
www.elsevier.com/locate/jpowsour

Analytical TEM study of Pt particle deposition in the proton-exchange membrane of a membrane-electrode-assembly

Tomoki Akita*, Akira Taniguchi, Junko Maekawa, Zyun Siroma, Koji Tanaka, Masanori Kohyama, Kazuaki Yasuda*

National Institute of Advanced Industrial Science and Technology, AIST Kansai, Midorigaoka 1-8-31, Ikeda, Osaka 563-8577, Japan

Received 30 September 2005; accepted 12 October 2005
Available online 18 January 2006

Abstract

A single cell of a PEMFC with PtRu/C anode and Pt/C cathode catalysts after an acceleration test in which constant high potential was applied to the cathode was observed by analytical TEM to investigate the structural changes in electrocatalysts and the proton-exchange membrane (PEM) at a micro- and nano-scale. A cross-sectional specimen of a membrane-electrode-assembly (MEA) was successfully prepared for TEM observation by using an ultramicrotome. A thin area of the electrode catalyst layer and the PEM were observed at a nano- and atomic-scale. The interface between the catalyst layer and the PEM was also observed. The results showed that large Pt particles of about 10–100 nm were formed in the PEM after an acceleration test in which a constant potential was applied. This result indicates that Pt dissolved and diffused, and Pt crystals grew in the PEM. The distribution of Pt particles in the PEM depended on the kind of gas supplied for cathode.

Keywords: PEMFC; Fuel cell; Electrocatalyst; TEM; Degradation

1. Introduction

Proton-exchange membrane fuel cells (PEMFCs) are attractive low-emission power sources for electrically powered vehicles and distributed power generation [1]. Small PEMFCs (micro-fuel cells) have also been developed as power sources for portable equipment such as laptop computers, cellular phones, and so on [2]. Reliability and lifetime are the most important issues for practical use of such power sources. However, the mechanisms of the deterioration of PEMFC are not well understood. Particularly, the structural changes in the electrocatalyst and membrane in fuel cells at a microscopic scale are not well investigated. Thus, it is important that we determine the mechanisms of degradation under various operating conditions at a micro- and nano-scale.

In this work, a membrane-electrode-assembly (MEA) in a single cell of a PEMFC after accelerated degradation tests was observed by analytical transmission electron microscopy (TEM). Many detailed studies have been conducted to determine the structure of the electrocatalyst or membrane itself by using electron microscopy at a microscopic scale [3–5], and there have also been some reports on the structure of the cell for practical operation [6–11]. It is important that we observe the structure of the electrocatalyst, proton-exchange membrane (PEM), and the interface between the electrocatalyst and the PEM in MEA under various operating conditions to elucidate the mechanism of degradation. In our previous report, degradation caused by fuel starvation was investigated by analytical TEM [12]. We noted the dissolution of Ru from the PtRu/C electrocatalyst at the anode, and the growth of particles at both the anode and cathode. In this study, after acceleration tests in which a constant high potential was applied to the cathode, the MEA was observed by TEM to investigate structural changes in electrocatalysts and the PEM at a micro- and nano-scale. Analytical TEM is very advantageous because it can reveal the spatial distributions of components even for complicated functional materials, and can be used to analyze the composition of a local area at a nano- or atomic-scale. It is an indispensable tool for analyzing functional materials such as fuel cells which have a complicated structure at the nano-scale. Although it is difficult to prepare sufficiently thin specimens from such

* Corresponding authors. Tel.: +81 727 51 9732/9653; fax: +81 727 51 9629.
E-mail addresses: t-akita@aist.go.jp (T. Akita), k-yasuda@aist.go.jp (K. Yasuda).

0378-7753/$ – see front matter © 2005 Elsevier B.V. All rights reserved.
doi:10.1016/j.jpowsour.2005.10.111

complicated functional materials for TEM observation, cross-sectional specimens of a membrane-electrode-assembly (MEA) were successfully prepared for TEM observation by using an ultramicrotome. Accelerated degradation tests were carried out by applying high potential to the cathode while supplying N_2 gas or air. The structure of the cell after the acceleration test was investigated by TEM.

2. Experimental

Electrodes for the PEMFC were prepared from a 10 wt.% carbon black-supported platinum electrocatalyst (Johnson Matthey) for the cathode and 30 wt.% Pt/C/15 wt.% Ru/C electrocatalyst (Johnson Matthey) for the anode and a Nafion® solution (5 wt.% solution, E.I. DuPont de Nemours and Company). Catalyst ink was prepared by adding Nafion® solution with isopropyl alcohol to the electrocatalyst powder. The resulting ink was applied to a polytetrafluoroethylene (PTFE) sheet, and then dried and transferred to a proton-exchange membrane, Nafion® (7 mil-thick and 1100 EW sulfonic acid form, DuPont) by hot-pressing to produce a membrane-electrode-assembly. The Nafion® content of the electrodes was 15 wt.%. The Nafion® membrane pretreated with hydrogen peroxide and 1 mol/l H_2SO_4 aqueous solution. Wet-proofed carbon paper (TGPH 060, Toray) was used as gas diffusion backing. The accelerated degradation test was performed using a single cell. The details of the configuration of the cell have been described previously [12]. Potential holding experiments were carried out in a single circular cell (10 cm^2) made from titanium without a precious metal coating to avoid the effect of cell material corrosion. The flow field was a conventional parallel channel design. A constant potential was applied to the cathode against the anode as a reference hydrogen electrode (RHE) by an HA-151 Potentiostat/Galvanostat while pure N_2 or pure air was supplied for the cathode and pure H_2 was supplied for the anode at 353 K. A potential of 1.0 V was applied for 30, 87 h in these experiments. The cell was maintained at 353 K and the operating pressure was atmospheric. Gases were humidified at the same temperature as the cell and fed to each electrode. The electrochemically active surface area was evaluated from the hydrogen desorption charge of a cyclic voltammogram using an electrochemical analyzer (BAS100B/W).

The cross-sectional specimen for TEM observation was prepared by ultramicrotomy. The carbon paper was removed from the single cell and the MEA was cut into pieces that measured about 1.5 mm × 3.0 mm × 0.2 mm using a razor. A small piece was embedded in epoxy resin (EPON 812 RESIN) and dried for a few hours. A piece of the MEA was sliced by an ultramicrotome (Leica ULTRACUT UCT) using a diamond knife at room temperature. The thickness of the sample was about 30–60 nm. The sliced specimen was supported on a conventional φ3 mm Cu mesh with a carbon micro-grid. The TEM observations were performed using a JEOL JEM-3000F transmission electron microscope equipped with a Thermo Noran energy dispersive X-ray spectroscopy (EDS) system. The TEM was operated at an accelerating voltage of 300 kV. Observations were also conducted at room temperature without a cooling stage. The regions of the anode, cathode, membrane and epoxy resin were identified by EDS measurement in the TEM image. We could distinguish the membrane from the epoxy resin by noting the peaks of fluorine and oxygen in EDS spectra. The epoxy resin shows X-ray signals corresponding to oxygen without a peak for fluorine, while strong fluorine peaks are seen in the PEM region.

3. Results and discussion

Fig. 1a shows the time-dependence of the electrochemically active surface area of cathode Pt catalyst during the application of a constant voltage of 0.8 V or 1.0 V versus RHE under air. The value is given as a percentage of the initial value. The active surface area decreased with the duration of testing and also depended on the applied voltage. The decrease in the surface area was almost saturated at around 100 h for 1.0 V. The prolonged holding of the cathode at 1.0 V versus RHE, which reflects holding near the open circuit potential of the PEMFC with negligible oxygen reduction current, resulted in large cathode degradation. Although this decrease in the electrochemically active surface area is caused by sintering of platinum particles, a small amount of platinum dissolves out of cathode catalyst layer as described below.

Fig. 2a shows a low magnification TEM image around the interface between the Pt/C cathode and PEM after 1.0 V was applied for 87 h under air. The lower left side of the TEM image is the Pt/C catalyst layer and Pt particles are seen as dark contrast. The upper right side is the PEM region, and uniform contrast is seen at this magnification. Fig. 2b and c shows TEM images of the PEM approximately 10 μm from cathode layer and the interface between the PEM and the PtRu/C anode layer, respectively. The PEM is often torn during sample preparation when the specimen is thin, and it is difficult to observe the whole region from the cathode to the anode. One noticeable feature is that large Pt particles appeared in the PEM near the Pt/C electrocatalyst layer. The Pt particles are large compared to the Pt particles in the electrocatalyst. The Pt particles observed in the PEM are 10–100 nm while those in the electrocatalyst are 2–5 nm. These

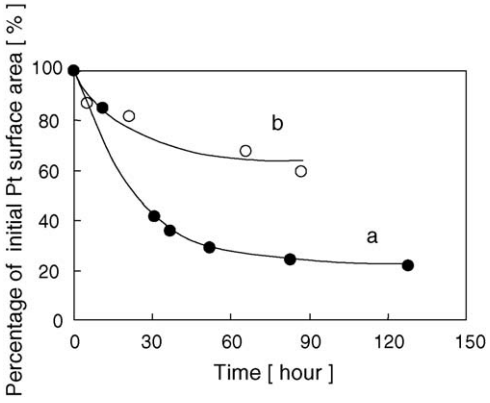

Fig. 1. Electrochemically active surface area of Pt presented as a percentage of the initial value. Cathode potential was held potentiostatically at (a) 1.0 V, (b) 0.8 V vs. RHE.

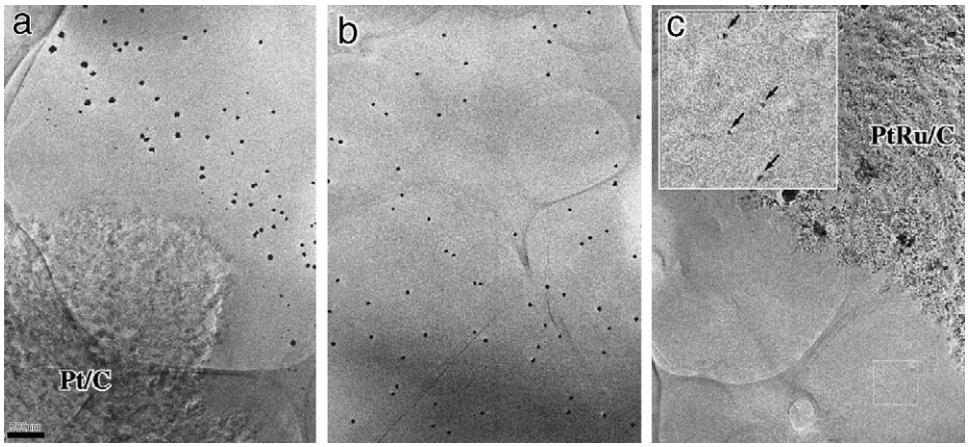

Fig. 2. Cross-sectional TEM images of a MEA after 1.0 V was applied for 87 h. (a) TEM image near the interface between the cathode catalyst layer and the PEM, (b) TEM image of the PEM 10 μm from the cathode layer, (c) TEM image near the interface between the anode catalyst layer and the PEM.

large Pt particles are also observed in Fig. 2b, which was taken far from the cathode layer in the PEM. The Pt particles gradually decrease in size depending on the distance from the cathode layer. Small Pt particles are observed even in the PEM near the anode side, as shown in Fig. 2c. The enlarged TEM image from the area indicated by the white rectangle is shown in Fig. 2c and the Pt particles are indicated by arrows. The Pt atoms seem to diffuse from the cathode to the anode layer during applying constant potential.

Fig. 3 shows the EDS spectrum obtained from a Pt particle in the PEM. The particle mainly consists of platinum. A peak for copper appears as background signal from the Cu-grid supporting the sample. Carbon and fluorine are detected from the PEM in the measurement area. Small peaks of potassium and iron are also detected as impurities. The peak of sulfur overlaps the minor peak of Pt and it is difficult to distinguish the peaks when the signal is weak. It is also difficult to detect the sulfur peak since sulfur is easily desorbed by irradiation with a high-energy electron beam.

Fig. 4 shows high-resolution TEM (HRTEM) images and electron diffraction patterns from the Pt particle observed in the PEM after the test corresponding to the sample shown in Fig. 2. The Pt particle has a complicated shape as shown in Fig. 4a and d. It appears as if some small Pt particles aggregate into a large Pt particle. Interestingly, the corresponding diffraction pattern indicates that the Pt particle almost consists of a single crystal. Fig. 4b and e shows diffraction patterns corresponding to the TEM images in Fig. 4a and d, respectively. They are single crystalline diffraction patterns from the ⟨1 1 0⟩ zone axis and ⟨1 2 3⟩ zone axis for a face centered cubic (fcc) structure. Enlarged HRTEM images of part of these Pt particles are shown in Fig. 4c and e. The HRTEM images also show lattice fringes and a well-ordered crystalline structure. Fig. 4c shows the lattice image from the ⟨1 1 0⟩ direction, and the {1 1 1} and {2 0 0} crystal planes are clearly observed. The {1 1 1} plane is seen in Fig. 4f, as observed from the ⟨1 2 3⟩ direction.

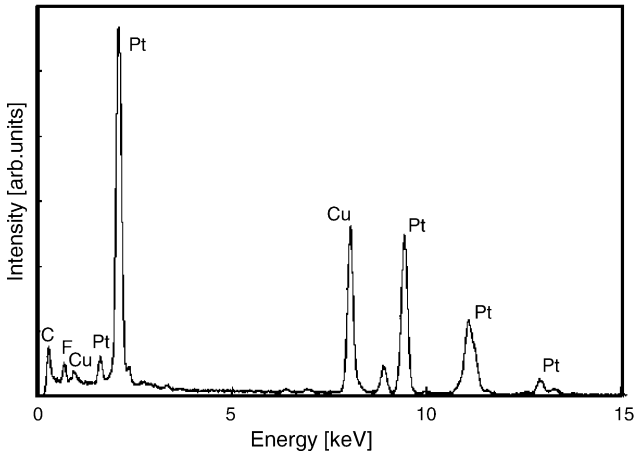

Fig. 3. EDS spectrum obtained from a Pt aggregates in PEM.

Aggregates of Pt particles were often observed in the electrocatalyst layer even for the MEA before the degradation test. The Pt aggregates in the electrocatalyst layer generally show a poly-crystalline diffraction pattern as shown in Fig. 5. It appears as though some small Pt particles aggregate into a large particle. The structure of Pt particles in PEM is apparently different from that in the electrocatalyst layer. The Pt particles in the PEM shown in Fig. 4 seem to grow atomically without the coalescence of small particles. The surface of the Pt particle indicates curvature, and low index facets are observed in the equilibrium crystal are not seen. This means that the interfacial energy of the Pt particle in the PEM is different from that in a vacuum. The growth of the Pt particle occurs under restricted conditions in the PEM. These Pt particles are considerably larger than the size of the ionic cluster in the PEM [13].

Fig. 6 shows low-magnification TEM images around the interface between the Pt/C cathode and the PEM after 1.0 V was applied for 87 h with N_2 gas supplied for the cathode. Fig. 6b and c shows TEM images of the PEM approximately 15 μm from the cathode layer and the interface between the PEM and the PtRu/C anode layer, respectively. There are a few small particles in the PEM, as indicated by arrows in Fig. 6b, and Pt particles are not detected near the PtRu/C layer, as shown in Fig. 6c. The dis-

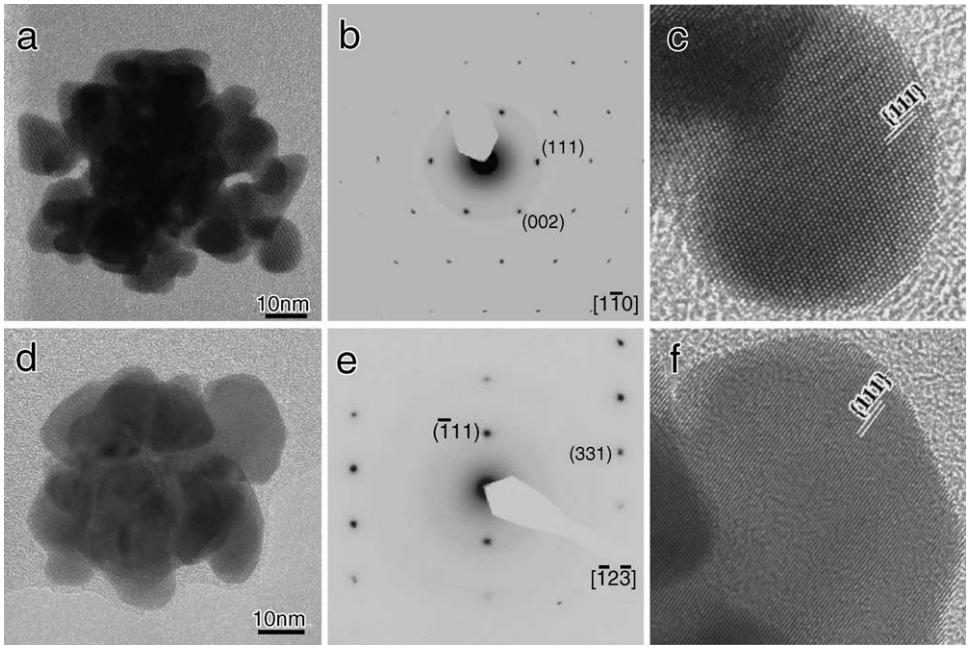

Fig. 4. TEM images and electron diffraction patterns of Pt particles in the PEM. (a and d) Low-magnification TEM images of Pt particles in the PEM, (b and e) corresponding electron diffraction patterns of the Pt particles, and (c and f) HRTEM images of the Pt particles.

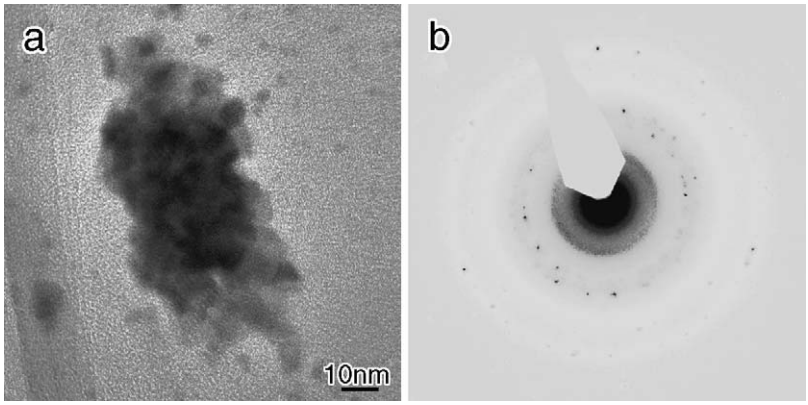

Fig. 5. (a) TEM image of a Pt aggregate in the catalyst layer and (b) the corresponding electron diffraction pattern.

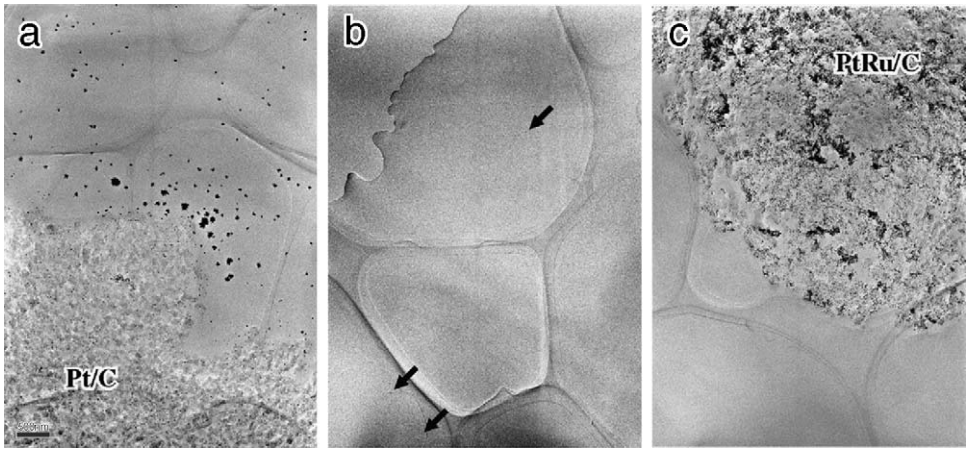

Fig. 6. Cross-sectional TEM images of a MEA after 1.0 V was applied for 87 h with N_2 supplied for the cathode. (a) TEM image near the interface between the cathode layer and the PEM, (b) TEM image of the PEM 15 μm from the cathode catalyst layer, (c) TEM image near the interface between the anode catalyst layer and the PEM.

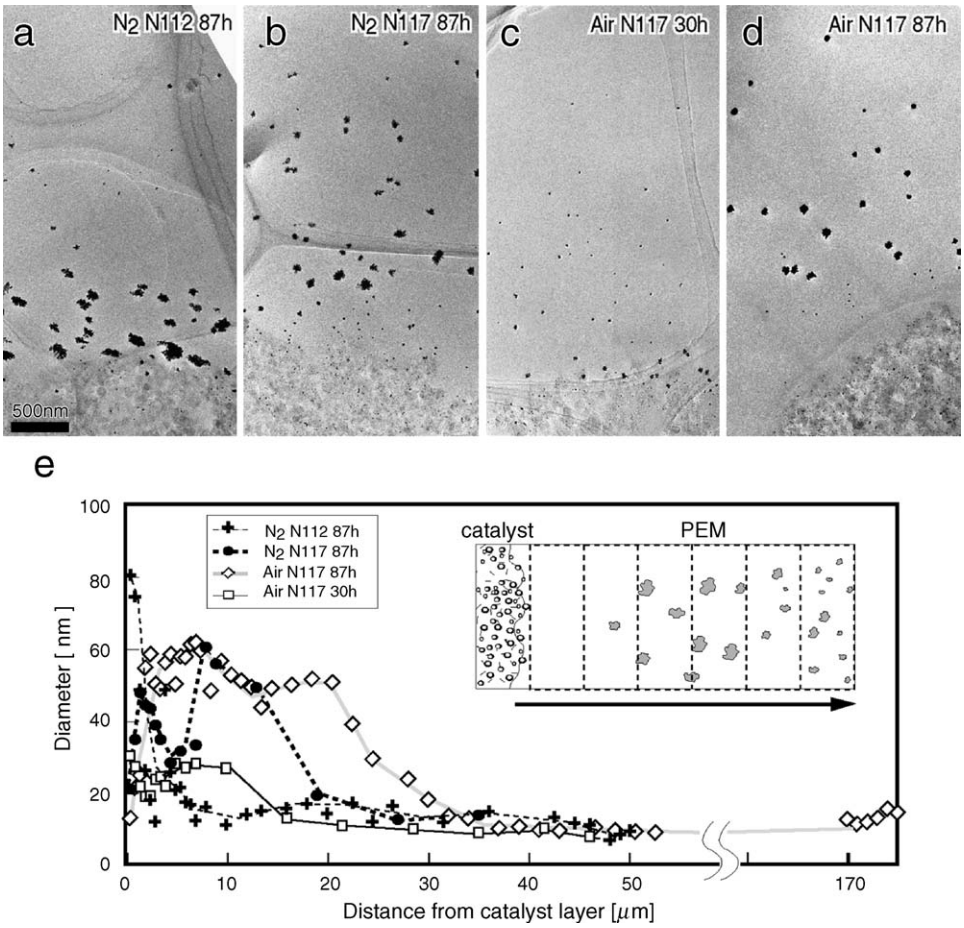

Fig. 7. TEM images of the interface between the cathode and PEM after acceleration tests and the size distribution of Pt particles in the PEM. 1.0 V vs. RHE for the cathode with N_2 gas supplied for 87 h (a) using Nafion® 112, (b) using Nafion® 117, and with air supplied (c) for 30 h using Nafion® 117, and (d) for 87 h. Size distribution of Pt particles in the PEM (e).

tribution of Pt particles in the PEM depends on the kind of gas supplied for the cathode.

The results of tests under various conditions are summarized in Fig. 7. These TEM images were taken after acceleration tests in which we varied the gas supplied for the cathode, the thickness of the PEM and the duration of testing. Fig. 7a–c shows TEM images after 1.0 V was applied for 87 h with N_2 supplied for the cathode. Based on a comparison with Fig. 2, platinum deposition is restricted to near the cathode catalyst layer. The dependence of the platinum distribution on the membrane thickness was investigated using a thinner membrane, Nafion® 112, with a thickness of 50 μm, with N_2 supplied for the cathode. With Nafion® 112, platinum deposition in the electrolyte membrane was seen closer to the catalyst layer, as shown in Fig. 7a compared to Fig. 7b. The mean diameter of Pt particles versus the distance from the electrocatalyst layer is summarized in Fig. 7e. This graph shows the mean diameter, and does not indicate the amount or density of Pt in the PEM. The mean diameter was measured from the each specific region of TEM images about 1 μm in width perpendicular to the catalyst layer, as illustrated in the inset in Fig. 7e. Large particles exist near the catalyst layer and few Pt particles appear far from the catalyst layer when N_2 gas was supplied for the cathode. The distribution of Pt particles also depends on the thickness of the PEM. Pt particles were distributed near the cathode layer when a thin PEM was used, as seen in Fig. 7a. When air was supplied for the cathode for 87 h, the Pt particles almost reached the anode layer through the PEM, as shown in Fig. 2.

Fig. 8 shows a schematic drawing of the possible growth process of Pt particles in the PEM. A Pt particle is almost a single crystal, as shown in Fig. 4. This result indicates that the Pt aggregates in the membrane are not formed by the migration and coalescence of Pt particles from the catalyst layer. The Pt particles seem to form nuclei and grow atomically by the deposition of dissolved Pt ionic species. The applied voltage of 1.0 V is sufficient to dissolve some of the Pt particles to Pt ions. The single crystal generally shows isotropic growth in the liquid or vapor phase under equilibrium. In such a case, atoms will be uniformly supplied from the surroundings to the nuclei, and an isotropic equilibrium crystalline shape will be observed depending on the surface energy, which is well known as Wulff construction. However, in the PEM, the supply of Pt ions to the nuclei is not uniform because of the microscopic phase separation, which results in the formation of ionic clusters. Furthermore, the overpotential of Pt deposition on the nuclei may be large (i.e. far from equilibrium), which generally inhibits layered deposition.

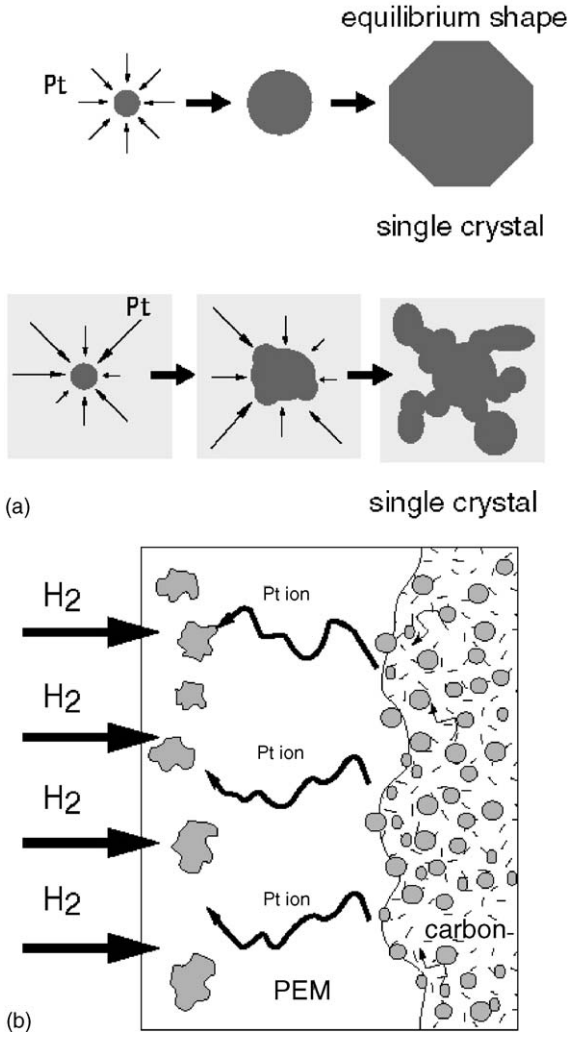

Fig. 8. Schematic drawings of the possible growth process of Pt particles in the PEM.

These possibilities may explain the complicated shape of the Pt particles shown in Fig. 4a and d. Concerning the distribution of Pt particles in the PEM, the spatial distribution of Pt particles appears to be related to the hydrogen distribution in the PEM crossover from the anode through the PEM, as shown in Fig. 8b. In the MEA for PEMFC, it has been reported that some of the supplied gas such as hydrogen traverses the membrane [14,15]. Pt ionic species are dissolved into the PEM from the catalyst layer by the applied high potential. Pt ionic species dissolved in the PEM then diffuse through the PEM. The form of the Pt ionic species is unknown. Pt cation can diffuse due to a concentration gradient. An anionic Pt complex formed with fluoride or sulfonate anion formed by membrane degradation or a chloride anion impurity can also migrate by a potential gradient in the PEM under operating conditions of the cell. They are reduced by hydrogen gas coming from the anode, form nuclei and grow into large particles. Interestingly, Fig. 2a shows that the Pt particles are not strictly distributed along the interface of the cathode layer but rather appear in a straight line. The distribution of Pt particles parallels the macroscopic-scale interface between the PEM and the catalyst layer. This suggests that the Pt particles are distributed depending on the hydrogen concentration in the PEM. Hydrogen crossover through the membrane increases with decreasing membrane thickness, since the concentration gradient within the membrane increases. The distribution of Pt particles in the PEM depends on the concentration of hydrogen in the membrane, as shown in Fig. 7.

In the case of a cathode with air, the oxygen concentration near the cathode interface is high and the hydrogen concentration is low. Under these conditions, it may be difficult for a platinum nucleus to be generated by reduction with hydrogen since a very small platinum nucleus might be unstable with a high potential (mixed potential composed of dissolved hydrogen and oxygen) under such oxygen-rich conditions. Therefore, the Pt ions can diffuse longer toward the anode before nucleus generation occurs under air for the cathode. We are currently studying the details of the mechanism of the aggregation of Pt in the PEM.

4. Conclusion

The structure of a MEA after the application of a potential was successfully observed by analytical TEM at a nano- and atomic-scale. The results indicated that

(1) Large Pt aggregates are observed in the PEM by an acceleration test in which potential is applied to the cathode.
(2) The Pt aggregates formed in the PEM have a well-ordered crystalline structure.
(3) The distribution of Pt particles depends on the concentration of gases in the PEM.

Acknowledgements

This work received financial support from the new Energy and Industrial Technology Development Organization (NEDO) as part of the Research and Development of Polymer Electrolyte Fuel Cell Technology Project directed by the Ministry of Economy, Trade and Industry (METI), Japan.

References

[1] P. Costamagna, S. Srinivasan, J. Power Sources 102 (2001) 253–269.
[2] C.K. Dyer, J. Power Sources 106 (2002) 31–34.
[3] R.M. Stroud, J.W. Long, K.E. Swider-Lyons, D.R. Rolison, Microsc. Microanal. 8 (2002) 50–57.
[4] V. Radmilovic, H.A. Gasteiger, P.N. Ross Jr., J. Catal. 154 (1995) 98–106.
[5] Z. Porat, J.R. Fryer, M. Huxham, I. Rubinstein, J. Phys. Chem. 99 (1995) 4667–4671.
[6] D.A. Blom, J.R. Dunlap, T.A. Nolan, L.F. Allard, J. Electrochem. Soc. 150 (2003) A414–A418.
[7] M. Schulze, T. Knöri, A. Schneider, E. Gülzow, J. Power Sources 127 (2004) 222–229.
[8] M. Schulze, A. Schneider, E. Gülzow, J. Power Sources 127 (2004) 213–2219.
[9] J. Xie, D.L. Wood III, K.L. More, P. Aatanassov, R.L. Borup, J. Electrochem. Soc. 152 (2005) A020–A1011.
[10] M.S. Wilson, F.H. Garzon, K.E. Sickafus, S. Gottesfeld, J. Electrochem. Soc. 140 (1993) 2872–2877.

[11] J. Yu, T. Matsuura, Y. Yoshikawa, M.N. Islam, M. Hori, Phys. Chem. Chem. Phys. 7 (2005) 373–378.
[12] A. Taniguchi, T. Akita, K. Yasuda, Y. Miyazaki, J. Power Sources 130 (2004) 42–49.
[13] H.L. Yeager, A. Steck, J. Electrochem. Soc. 128 (1981) 1880–1884.
[14] K. Broka, P. Ekdunge, J. Appl. Electrochem. 27 (1997) 117–123.
[15] S. Cleghorn, J. Kolde, W. Liu, Handbook of fuel cells—fundamentals, technology and applications, in: W. Vielstich, H.A. Gasteiger, A. Lamm (Eds.), Fuel Cell Technology and Applications, vol. 3, John Wiley and Sons, 2003, p. 566.